SURFACE TITRATION OF COLLOIDAL α-ALUMINA

J.W. Ntalikwa

Department of Chemical and Process Engineering, University of Dar es Salaam,
P.O. Box 35131 Dar es Salaam, Tanzania

T *he surface charge density (σ_o) of colloidal alumina (α-Al_2O_3) suspended in 1:1 electrolytes (NaCl, NaNO$_3$, CsCl and CsNO$_3$) at different electrolyte concentration (c_0) was determined using acid-base titration. The data were described in terms of the Triple Layer Model (TLM) of electric double layer. It was observed that the polarity of σ_o could be varied through a point of zero charge (PZC) by varying the pH of the suspension. The PZCs were observed to occur at pH = 7.8 ± 0.1, 7.6 ± 0.2, 8.5 ± 0.1 and 8.3 ± 0.1 in NaCl, NaNO$_3$, CsCl and CsNO$_3$, respectively. It was concluded that the TLM adequately describes the titration data (within ±10%) in the pH and c_0 range of $10^{-4} \leq c_0 \leq 0.1$ M, respectively.*

Keywords: *surface charge density, acid-base titration, Triple Layer Model, colloid, alumina.*

INTRODUCTION

The surface charge density (σ_o) and potential (ψ_o) of oxides do influence interactions at the oxide/liquid interface. Other parameters such as the nature of the surface ionizable groups, concentration and composition of the dispersion medium also play a great role in characterising the interactions at the oxide/liquid interface. The interactions at the mineral oxide interface affect many geo-chemical processes such as the uptake, transport and release of adsorbed contaminants, mineral dissolution and precipitation, various redox reactions and the colloidal stability of colloidal oxide dispersions (Stumm and Morgan, 1981; Cesarano et al., 1988; Dzombak et al., 1990). Therefore, experimental knowledge of these properties allows a variety of model predictions to be evaluated as part of the characterisation process of a colloidal oxide.

It has been established that in the presence of water, the surfaces of mineral oxides, especially those of Al, Fe and Si are generally covered with hydroxyl groups (Smit and Holten, 1980; James and Parks, 1982; Hayes et al., 1991; Katz and Hayes, 1995). Surface hydration and dissociation of these groups, results in a pH dependent surface charge density that is amenable to measurement by acid-base titration of dispersed material. The surface charge density determined by such methods (σ'') is essentially a relative or analytical one. This is because the value prior to addition of reagents to the dispersed material (σ'' at the point of zero titration) is often unknown and difficult to establish. However, there are various procedures (Hunter, 1996; Lyklema, 1995) that can be used to transform measured values of σ'' to surface charge density (σ_o).

In this work, surface properties of α-alumina are reported. The properties of this mineral oxide appear to be very limited in literature despite that those of a similar material (γ-alumina) have been reported by many authors (Huang and Stumm, 1973; Wiese and Healy, 1975; Sprycha, 1989a, 1989b; Mustafa et al., 1998). These two materials may have different surface characteristics arising from their differences in their crystal structure.

The measurements of σ'' of α-alumina in four electrolytes (NaCl, NaNO$_3$, CsCl and CsNO$_3$) at various concentrations were made using automated acid-base titration equipment. The titration data were used to estimate σ_o. The values of σ_o were then compared with those generated using a Triple Layer Model as formulated by Yates et al. (1974) and subsequently modified and used by Davis et

al. (1978), Davis and Leckie (1978, 1980), Lutzenkirchen *et al.* (1995) and Lutzenkirchen (1998, 1999).

EXPERIMENTAL

Materials and Methods

Materials: α-alumina (AKP 30 grade) obtained from Mandoval Zirconia sales Ltd, UK, was used as obtained. The chemical analyses provided by the manufacturer (Table 1) suggest that the material is of high purity.

Specific Surface Area: The specific surface area was determined using nitrogen gas adsorption and the Brunauer, Emmett and Teller (BET) method. The ASAP 2000 System Micromeritics Instrument, USA was used.

Particle Density: The particle density was determined by pycnometry using water as the dispersion medium.

Chemicals: All chemicals were of analytical reagent grade (obtained from either Fisons Co. Ltd, Acro Organics Ltd. UK, or Fisher Scientific UK). Water was produced by reverse osmosis, ion exchange, carbon adsorption and microfiltration of the local supply to pH and conductance of 5.5-5.8 and 0.7-1.2 $\mu S\ cm^{-1}$, respectively. Electrolytes were prepared by dissolving known amounts of salt in water. Electrolyte solutions were prepared every two weeks and allowed to stand at least one day (24 hours) prior to use. Titrants HCl, HNO_3 and NaOH were obtained as 1.0 M standard solutions, whereas 1.0 M CsOH was made by dilution from a stock (50% w/w) CsOH.

Sample Preparation and Titration: Samples were prepared by dispersing 7.3 g air dry (6.9 g oven dry) of α-alumina powder in 50 ml of electrolyte solution inside thermostatted jacketed titration cells. Samples were left to stand for 24 hours. Titrations were performed using high precision syringes ($25 \pm 0.1\ \mu l$) adjusted by stepper motors (Hamilton PSD/2). Reagents were drawn into the syringes from large capacity reagent reservoirs and were delivered to samples via micro-bore tubing. Sample pH and temperature were monitored using single junction electrodes and platinum resistance thermometers, respectively. An inert atmosphere

Table 1: Chemical analysis of alumina specified by the manufacturer*

Component	Al_2O_3	Fe	Si	Cu	Mg	Na
% by weight	99.99	0.002	0.005	0.001	0.001	0.001

* Mandoval Zirconia sales Ltd, UK

above the sample was maintained using a supply of CO_2 free N_2. These facilities were controlled with a computer that also served as a data-logger. The system was configured to perform two titrations, essentially, in parallel. Duplicate samples were typically titrated, one with acid, the other with base, from their initial conditions at the point of zero titration (PZT).

The quantities of titrant added were adjusted using a predictor-corrector method to provide a uniform spread of experimental data points with respect to pH. Sample conditions were monitored following each addition of reagents. When sample pH was invariant with time it was assumed to be at equilibrium. Conditions were then recorded, another dose of titrant was then delivered and the process repeated until the pH reached a prescribed limits. A similar procedure was used for the titration of particle free electrolytes (blank titrations). Titrations were performed in the presence of various electrolyte salts (NaCl, $NaNO_3$, CsCl and $CsNO_3$ in the concentration range of $10^{-1}-10^{-4}$ M), using the conjugate acids and bases, from which they are derived, as titrants.

Data Analysis: Titration data were processed to provide continuous/semi-continuous functions of pH in relation to the cumulative addition of titrant for blank and corresponding sample titrations at each electrolyte concentration. This curve fitting was heuristic and adjusted to achieve a correlation coefficient (r) in the range $0.99 \leq r^2 \leq 1.00$ The functions obtained were used to calculate the corresponding cumulative titrant addition to blanks (N_{BL}) at corresponding pH points in the sample titration (N_{AL}). These values were then subtracted from those of the samples to compensate for any reagent interaction with surfaces of the cells and facilities therein to produce estimates of σ" at various pH from

$$\sigma'' = \frac{10^{-4} F(N_{AL} - N_{BL})}{m_p A_{sp}} \qquad (1)$$

Where, σ'' is analytical surface charge density (μCcm^{-2}), F is Faraday's constant ($Cmol^{-1}$), m_p is mass of the oxide (g), A_{sp} is the specific surface area of the oxide ($m^2 g^{-1}$) and N_{AL} and N_{BL} are moles of titrant for the sample and blank respectively, expressed in μmol.

In circumstances where relationships obtained from titration in various concentrations of the same electrolyte possessed a Common Intersection Point (CIP) (within an error of ± 0.2 pH units), the initial analytical surface charge density (σ_s) at that point was determined. In such situations, the absolute surface charge density (σ_0) was estimated from:

$$\sigma_0 = \sigma'' \pm \sigma_s \qquad (2)$$

RESULTS AND DISCUSSION

The material was found to have a specific surface area of 7200 ± 200 m^2 kg^{-1}. The density of the material was found to be 3900 ± 100 kg m^{-3}. The mean particle size on this basis is 0.40 ± 0.01 μm and agrees well with previously experimentally determined particle size (Ntalikwa et al., 2001) suggesting that the surface is largely non-porous.

σ'' as a Function pH NaCl and NaNO₃: The effect of pH on σ'' in various concentrations of NaCl produces a family of curves which appear to have

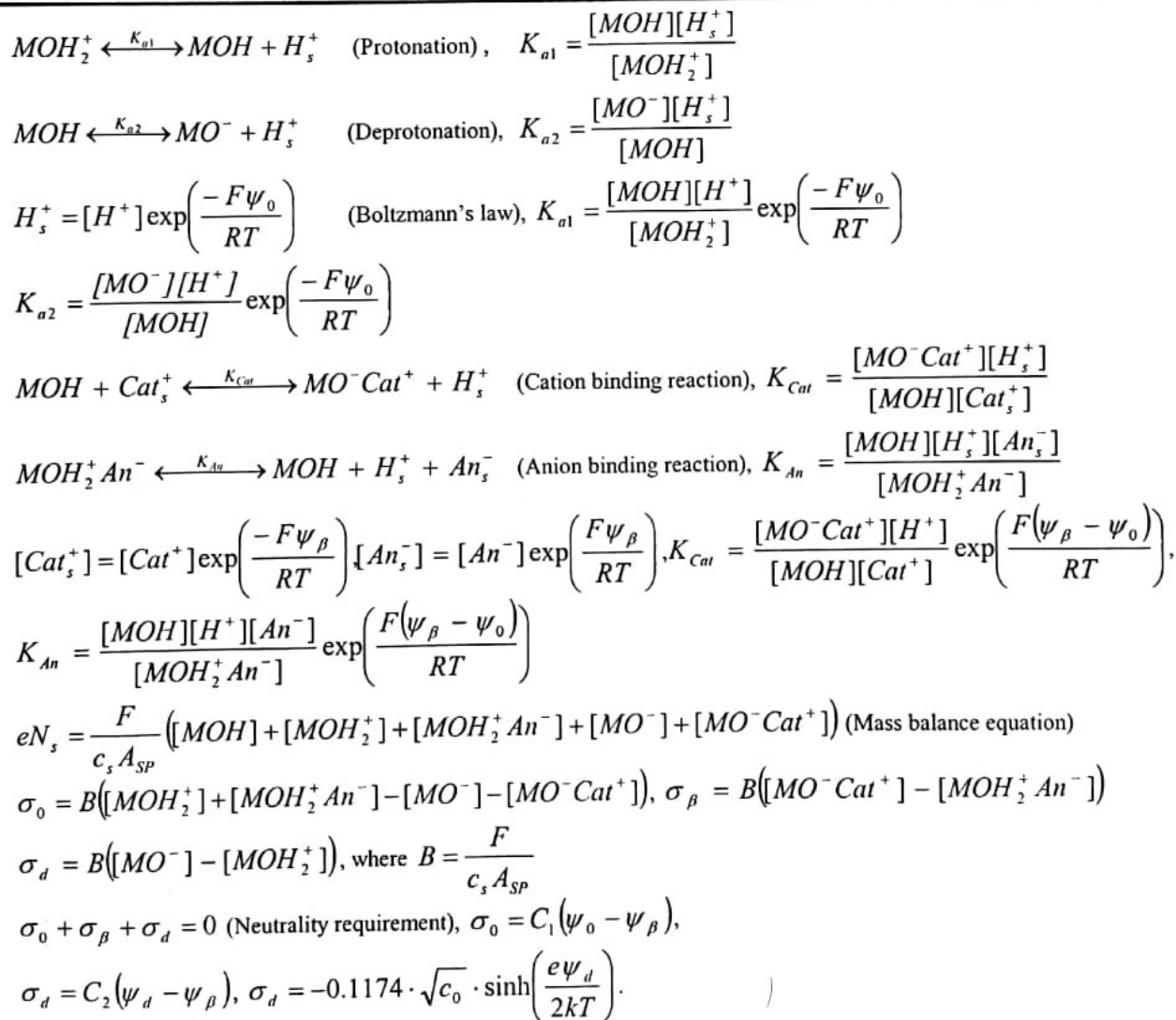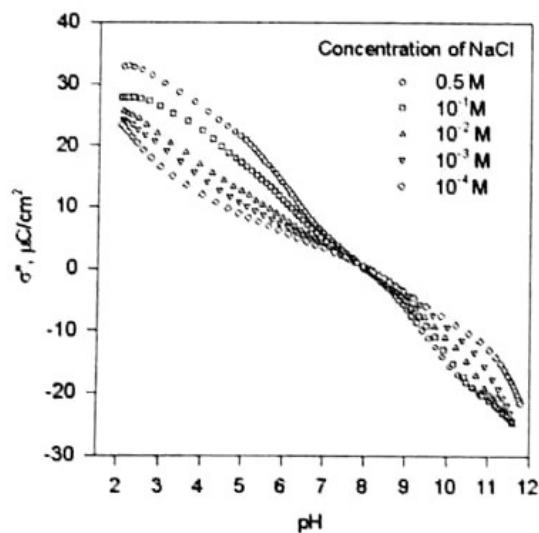**Table 2:** Summary of equations used in Triple Layer Model

$MOH_2^+ \xleftrightarrow{K_{a1}} MOH + H_s^+$ (Protonation), $\quad K_{a1} = \dfrac{[MOH][H_s^+]}{[MOH_2^+]}$

$MOH \xleftrightarrow{K_{a2}} MO^- + H_s^+$ (Deprotonation), $K_{a2} = \dfrac{[MO^-][H_s^+]}{[MOH]}$

$H_s^+ = [H^+]\exp\left(\dfrac{-F\psi_0}{RT}\right)$ (Boltzmann's law), $K_{a1} = \dfrac{[MOH][H^+]}{[MOH_2^+]}\exp\left(\dfrac{-F\psi_0}{RT}\right)$

$K_{a2} = \dfrac{[MO^-][H^+]}{[MOH]}\exp\left(\dfrac{-F\psi_0}{RT}\right)$

$MOH + Cat_s^+ \xleftrightarrow{K_{Cat}} MO^-Cat^+ + H_s^+$ (Cation binding reaction), $K_{Cat} = \dfrac{[MO^-Cat^+][H_s^+]}{[MOH][Cat_s^+]}$

$MOH_2^+An^- \xleftrightarrow{K_{An}} MOH + H_s^+ + An_s^-$ (Anion binding reaction), $K_{An} = \dfrac{[MOH][H_s^+][An_s^-]}{[MOH_2^+An^-]}$

$[Cat_s^+] = [Cat^+]\exp\left(\dfrac{-F\psi_\beta}{RT}\right) [An_s^-] = [An^-]\exp\left(\dfrac{F\psi_\beta}{RT}\right), K_{Cat} = \dfrac{[MO^-Cat^+][H^+]}{[MOH][Cat^+]}\exp\left(\dfrac{F(\psi_\beta - \psi_0)}{RT}\right),$

$K_{An} = \dfrac{[MOH][H^+][An^-]}{[MOH_2^+An^-]}\exp\left(\dfrac{F(\psi_\beta - \psi_0)}{RT}\right)$

$eN_s = \dfrac{F}{c_s A_{SP}}\left([MOH] + [MOH_2^+] + [MOH_2^+An^-] + [MO^-] + [MO^-Cat^+]\right)$ (Mass balance equation)

$\sigma_0 = B\left([MOH_2^+] + [MOH_2^+An^-] - [MO^-] - [MO^-Cat^+]\right), \quad \sigma_\beta = B\left([MO^-Cat^+] - [MOH_2^+An^-]\right)$

$\sigma_d = B\left([MO^-] - [MOH_2^+]\right)$, where $B = \dfrac{F}{c_s A_{SP}}$

$\sigma_0 + \sigma_\beta + \sigma_d = 0$ (Neutrality requirement), $\sigma_0 = C_1(\psi_0 - \psi_\beta),$

$\sigma_d = C_2(\psi_d - \psi_\beta), \quad \sigma_d = -0.1174 \cdot \sqrt{c_0} \cdot \sinh\left(\dfrac{e\psi_d}{2kT}\right).$

Table 3: Summary of TLM constants that gave best fits between predicted and experimental values of σ_0 for the salts investigated.

| Salt	c_0 (mol /l)	pK$_{a1}$	pK$_{a2}$	pK$_{Cat}$	pK$_{An}$	C_1 (Fm^{-2})	pφ
	0.5	6.3	9.3	9.00	6.60	1.90	0
NaCl	10^{-1}	6.3	9.3	8.30	7.30	1.50	0
	10^{-2}	6.3	9.3	7.00	8.00	1.18	0.3
	10^{-3}	6.3	9.3	6.00	9.00	1.00	0.3
	10^{-4}	6.3	9.3	5.00	10.00	0.80	0.3
	0.5	6.1	9.1	8.80	6.40	1.65	0
NaNO$_3$	10^{-1}	6.1	9.1	8.10	7.10	1.40	0
	10^{-2}	6.1	9.1	7.10	8.10	1.05	0
	10^{-3}	6.1	9.1	6.10	9.10	0.90	0
	10^{-4}	6.1	9.1	5.20	10.20	0.88	0
	0.5	7.0	10.0	9.90	7.50	1.60	-0.2
CsCl	10^{-1}	7.0	10.0	9.20	8.20	1.45	-0.2
	10^{-2}	7.0	10.0	8.20	9.20	1.25	-0.2
	10^{-3}	7.0	10.0	7.20	10.20	1.00	-0.2
	10^{-4}	7.0	10.0	6.50	11.50	0.85	-0.5
	0.5	6.8	9.8	9.70	7.30	1.45	-0.2
CsNO$_3$	10^{-1}	6.8	9.8	9.00	8.00	1.30	-0.2
	10^{-2}	6.8	9.8	8.00	9.00	1.02	-0.2
	10^{-3}	6.8	9.8	7.10	10.10	0.83	-0.3
	10^{-4}	6.8	9.8	6.00	11.00	0.80	-0.2

a CIP at pH = 7.8 ± 0.1 and $\sigma^* = 0.8 \pm 0.1$ $\mu C cm^{-2}$ (Figure 1). At pH above the CIP the curves spread more widely than at pH below it, whereas at a given pH the absolute values of σ^* appear to increase with increasing electrolyte concentration (c_0).

that above the CIP the positively charged surface is dominated by adsorbed anions whereas below the CIP the negatively charged surface is dominated by adsorbed cations. At pH ≤ 3 the concentrations of Cl$^-$ and NO$_3^-$ ions are enhanced due to the addition of HCl and HNO$_3$ in the NaCl and NaNO$_3$ systems, respectively. Likewise, in basic

Figure 1: σ^* as a function of pH in various concentrations of NaCl

The CIP of NaNO$_3$, occurs at pH = 7.6 ± 0.2 and $\sigma^* = 1.4 \pm 0.1$ $\mu C cm^{-2}$ (Figure 2). It is apparent
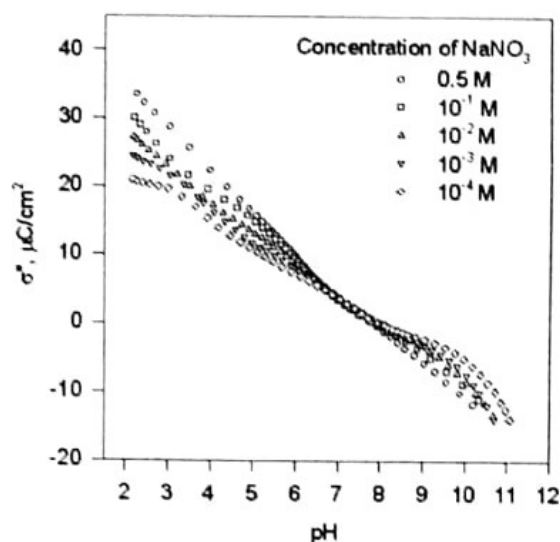
Figure 2 σ^* as a function of pH in various concentrations of NaNO$_3$.

conditions, (pH ≥ 10) the concentration of Na$^+$
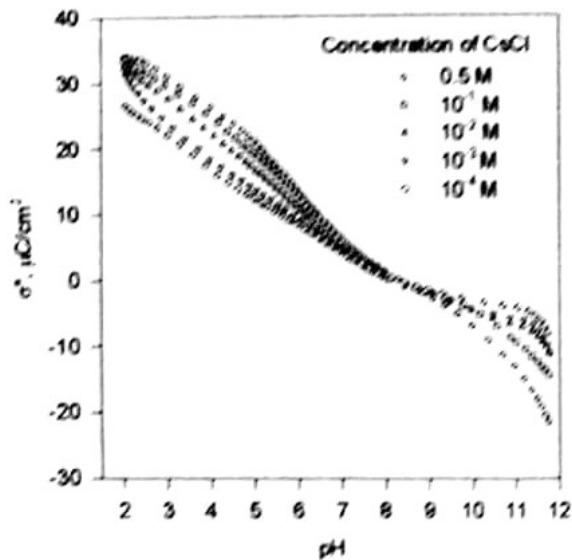
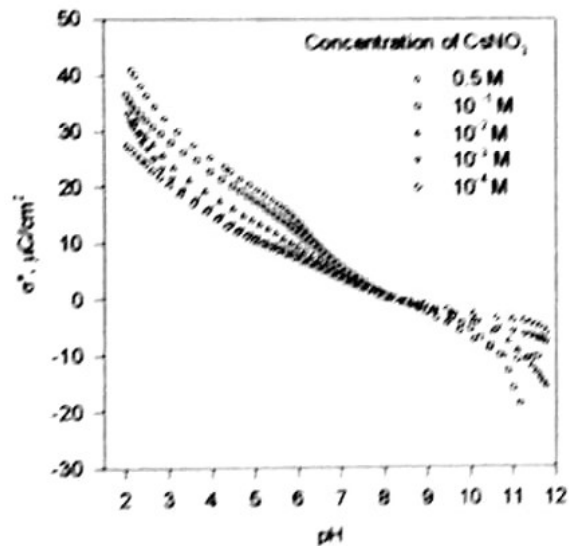**Figure 3:** σ'' as a function of pH in various concentrations of CsCl.

Figure 4: σ'' as a function of pH in various concentrations of CsNO$_3$

ions is very high due to the addition of NaOH. This suggests that the two systems should compare well in the range of $3 < pH < 10$. For instance, at pH 4, σ'' spans the range $12 \leq \sigma'' \leq 23$ μCcm^{-2} for NaCl (Figure 1) and it ranges $15 \leq \sigma'' \leq 20$ μCcm^{-2} for NaNO$_3$ (Figure 2). This suggests that the slightly smaller hydrated Cl$^-$ ion (radius 0.33 nm) favours formation of higher σ'' than the larger NO$_3^-$ ion (radius 0.34 nm).

σ'' as a Function pH CsCl and CsNO$_3$: The CIP in CsCl occurs at pH = 8.5 ± 0.1, $\sigma'' = -0.9 \pm 0.1$ μCcm^{-2} (Figure 3), whereas that in CsNO$_3$ occurs at pH = 8.3 ± 0.1, $\sigma'' = -0.2 \pm 0.1$ μCcm^{-2} (Figure 4). From Figs. 3 and 4 it can be noted that for $2 \leq pH \leq 12$, CsNO$_3$ generally shows higher values of σ'' than those of CsCl. Consequently, it appears for this system, NO$_3^-$ ions have significant impact on σ'' compared to Cl$^-$ ions.

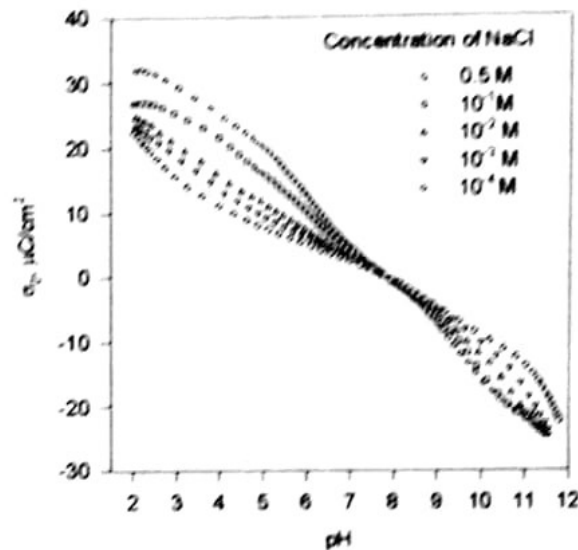Since all salts studied exhibited a CIP then equation 2 was used to transform σ'' to σ_0. The

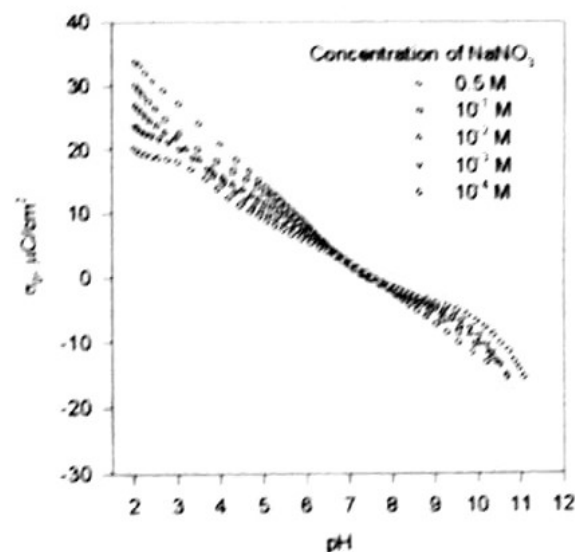**Figure 5:** σ_0 as a function of pH in various concentrations of NaCl.

Figure 6: σ_0 as a function of pH in various concentrations of NaNO$_3$

results are presented in Figure 5 through 8. From these it can be seen that they have similar features as those of Figure 1 through 4.

Model Predictions of σ_0: The theoretical prediction of σ_0 was made using the Triple Layer Model (TLM). The formulation of this model and the equations involved are similar to those presented by many authors (Davis *et al.*, 1978; Koopal *et al.*, 1987; Sprycha, 1989a, 1989b; Hayes *et al.*, 1991 and Zhang *et al.*, 1994). The principal equations are summarized in Table 2.

Estimation of Total Site Density (N_s) and Outer Capacitance (C_2): Despite the uncertainties in values of N_s and C_2 there is still no independent and accurate method of determining these constants so they are treated as adjustable parameters. In so doing the total number of adjustable parameters for the model is increased. In order to minimize their number, some may be assigned reasonable constant values. Experimental values of N_s were obtained by extrapolation of titration data (σ_0 versus pH curves) obtained at high c_0 to asymptotic values.

This provides a maximum value of σ_0 ($\sigma_{0, max}$) which is related to N_s. Performing this exercise for the curves of σ_0 versus pH at $c_0 \geq 0.1$ M, showed that $\sigma_{0, max}$ spans the range $35 \leq \sigma_{0, max} \leq 50$ μC

cm^{-2} for all electrolytes. This corresponds to N_s in the range $2.2 \leq N_s \leq 3.1$ sites nm^{-2} with an average value of 2.65 ± 0.45 sites nm^{-2}. This is within the range of 2–3 sites nm^{-2} reported by Katz and Hayes (1995) for α-Al$_2$O$_3$ and the average value is sufficiently close to 2.7 sites nm^{-2} reported from crystallographic estimates for the same oxide (Pivovarov, 1997). In the present work values of $N_s = 2.7$ sites nm^{-2} and $C_2 = 0.2$ Fm^{-2} were used throughout.

Estimation of Intrinsic Dissociation Constants pK_{a1} and pK_{a2}: Since alumina exhibited a PZC in every electrolyte investigated, then the PZC and ΔpK_a could be expressed as follows:

$$PZC = \frac{1}{2}\left(pK_{A1} - pK_{A2}\right) \tag{3}$$

$$\Delta pK_A = pK_{a2} - pK_{a1} \tag{4}$$

Equation 5 and 6, can be rearranged to give:

$$pK_{a1} = PZC - \frac{1}{2}\Delta pK_a \tag{5}$$

$$pK_{a2} = PZC + \frac{1}{2}\Delta pK_a \tag{6}$$

Schindler (1981) suggests that, a value of $\Delta pK_a = 3.0$ is appropriate for oxides such as TiO$_2$, Al$_2$O$_3$
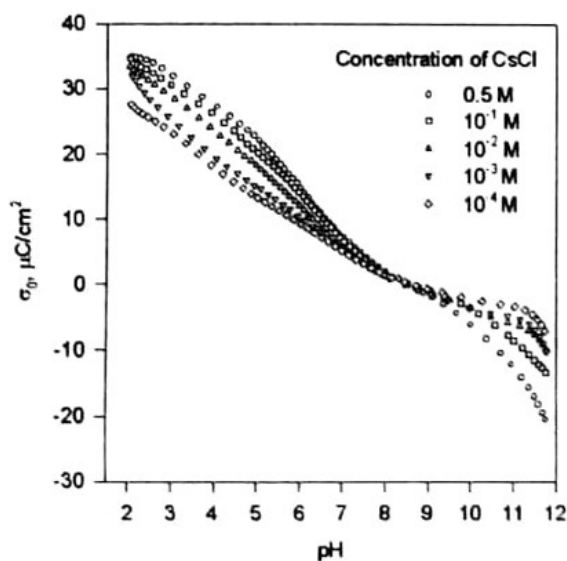

Figure 7: σ_0 as a function of pH in various concentrations of CsCl.

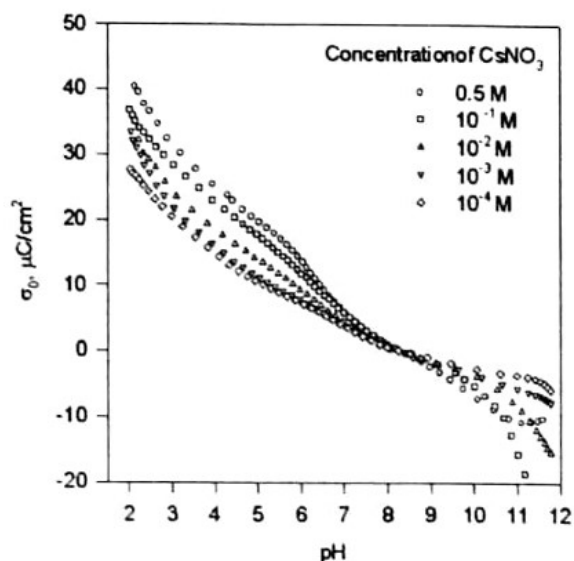**Figure 8:** σ_0 as a function of pH in various concentrations of CsNO$_3$

and FeOOH. For metal oxides, Huang (1981) and Hunter (1993) suggest a value of $\Delta pK_a = 3.0$. Hayes *et al.* (1991) were able to model different oxides with ΔpK_a in the range of $3.0 \leq \Delta pK_a \leq 4.0$. Katz and Hayes (1995) reported that, values of ΔpK_a in the range $2.0 \leq \Delta pK_a \leq 4.0$ resulted in a reasonable description of their titration data of α-Al_2O_3. In view of these observations, a value of $\Delta pK_a = 3.0$ was used here. Values of pK_{a1} and pK_{a2} were estimated using equation 5 and 6 with observed values of PZC.

Estimation of pK_{Cat} and pK_{An}

The values of pK_{Cat} and pK_{An} can be estimated from the following relationships:

$$pK_{Cat} = pK_{a2} + \log[Cat^+] + \log \phi_1 \qquad (7)$$

where,

$$\phi_1 = \frac{[MO^-]}{[MO^-Cat^+]} \exp\left(-\frac{e\psi_\beta}{kT}\right) \qquad (8)$$

and,

$$pK_{An} = pK_{a1} - \log[An^-] + \log \phi_2 \qquad (9)$$

where,

$$\phi_2 = \frac{[MOH_2^+ An^-]}{[MOH_2^+]} \exp\left(-\frac{e\psi_\beta}{kT}\right) \qquad (10)$$

Assuming that, the positively charged surface is essentially dominated by $[MOH_2^+]$ and $[MOH_2^+An^-]$ and the negatively charged surface is dominated by $[MO^-]$ and $[MO^-Cat^+]$. If these assumptions are adopted here, it follows that:

$$\frac{[MO^-]}{[MO^-Cat^+]} \approx \frac{[MOH_2^+]}{[MOH_2^+ An^-]} \approx 1.0 \qquad (11)$$

Substituting equation 11 into equation 8 and 10, the values of ϕ_1 and ϕ_2 appear to be equivalent (i.e. $\phi_1 = \phi_2 = \phi$, where ϕ is a function of ψ_β). Also, recognizing that $[Cat^+] = [An^-] = c_0$, equation. 7 and 9 can be re-written in the form:

$$pK_{Cat} = pK_{a2} - pc_0 - p\phi \qquad (12)$$

$$pK_{An} = pK_{a1} + pc_0 - p\phi \qquad (13)$$

where,

$pc_0 = -\log c_0$ and $p\phi = -\log \phi$.

In this work, $p\phi$ served as an adjustable parameter for estimation of pK_{Cat} and pK_{An}.

Solution of TLM Equations

The TLM equations were solved using the TK solver programme (Universal Technical Systems Inc., Rockford, IL, USA) release 3.32(1999). In this system, equations are viewed as rules and are iteratively solved using a Newton-Raphson method following assignment of initial guess values to one or more of the adjustable parameters.

For each set of adjustable parameters, 11 unknowns (i.e. σ_0, σ_β, σ_d, ψ_0, ψ_β, ψ_d, $[MOH]$, $[MOH_2^+]$, $[MO^-]$, $[MO^-Cat^+]$ and $[MOH_2^+An^-]$) were determined. Initial guess values $[MOH]$, $[MOH_2^+]$ and ψ_d were assigned as 0.15 mol/l, 10^{-4} mol/l and 0.01 V, respectively. Convergence to a solution was rapid. The adjustable parameters (C_1 and $p\phi$) were varied systematically to obtain agreement between predicted and experimental values of σ_0.

Indicator of Goodness of Fit and Sensitivity Analysis

The overall variance (V_Y) was used as the indicator of best fit between predicted and experimental values of σ_0. This was, defined as the sum of the squares of weighted residuals (*SOS*) divided by the degree of freedom (*DF*) (Dzombak and Morel, 1990; Hayes *et al.*, 1991; Katz and Hayes, 1995), i.e.

$$V_Y = \frac{SOS}{DF} = \frac{\sum\left(\frac{Y_i}{S_i}\right)^2}{N_P \cdot N_R - N_u} \qquad (14)$$

where,

Y_i = Residuals for each data point. In this work, $Y_i = (\sigma_0)_{calc}(i) - (\sigma_0)_{expt}(i)$.

S_i = Estimated error for each titration data point. This value is derived from the accuracy of pH measurement during titration. In this work, this error was estimated to be ± 0.02.

N_P = Number of data points.

N_R = Number of components for which both the total and the free concentration are known. Since there was only one component (i.e. H^+) for which both the total and free concentrations were known, then this parameter was always equal to 1.

N_u = Number of adjustable parameters. Since there were only two adjustable parameters, then this parameter was equal to 2.

Comparison of Experimental and Predicted Values of σ_0

The comparison between experimental and predicted values of σ_0 for α-alumina in various concentrations of NaCl are shown in Figures 9 through 12 from which the following general observations can be made:

a) The model predicts well (within ± 10%) the values of σ_0 in the concentration range of 10^{-4} $\leq c_0 \leq 10^{-2}$ M and pH range of 3< pH< 11. Above this range of c_0, the agreement between experimental and predicted values of σ_0 is generally not good (within ±15%).

b) σ_0 values below the PZC (negative charge) are generally not predicted well compared to those above it (positive charge) especially at high c_0 (≥ 0.1 M).

The discrepancies between experimental and predicted values of σ_0 at $c_0 > 10^{-2}$ M (observation (a)) may arise from the effects of high concentration of ions around the alumina particles.
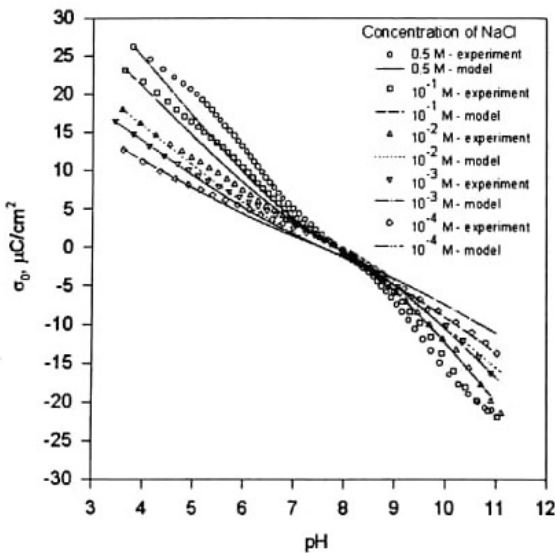

Figure 10: Comparison of experimental and predicted values of σ_0 at various concentrations of NaNO$_3$
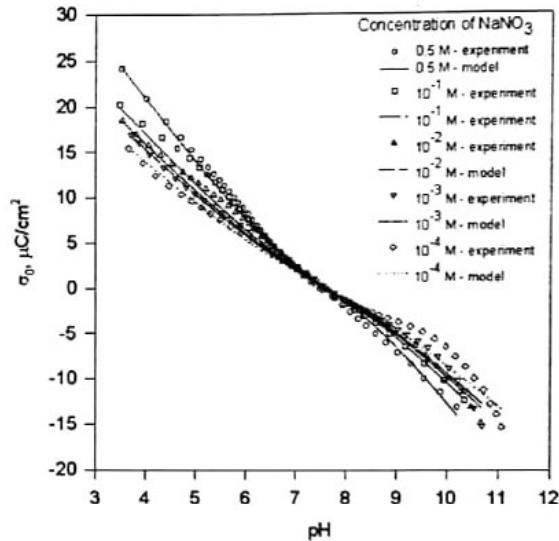

Figure 9: Comparison of experimental and predicted values of σ_0 at various concentrations of NaCl
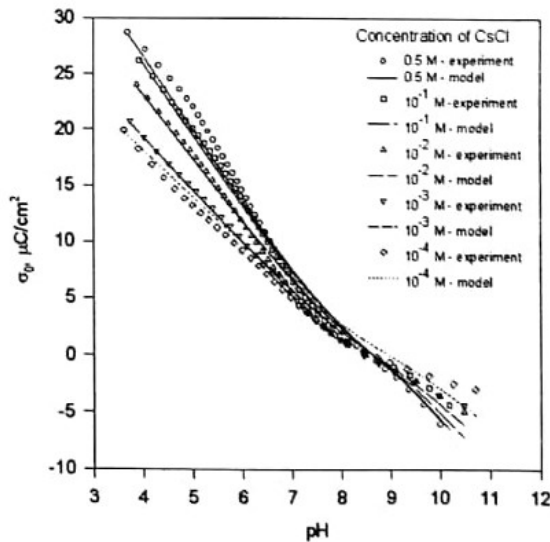

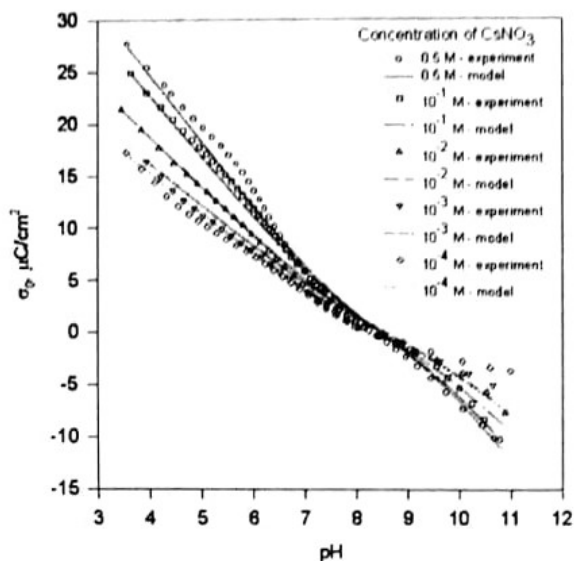**Figure 11:** Comparison of experimental and predicted values of σ_0 at various concentrations of CsCl

Figure 12: Comparison of experimental and predicted values of at various concentrations of CsNO3

Among of these is the discreteness of surface charge, which was not taken into account by the model. Furthermore, in this range of c_0, binding of electrolyte ions on the surface of the particle dominates and it may constitute a major fraction of the total σ_0. This suggests that, inappropriate description of the binding reactions may result in a significant lack of agreement between predicted and experimental values of σ_0. In the TLM suggested herein, the binding of electrolyte ions was taken into account through the intrinsic complexation dissociation constants (K_{Cat} and K_{An}).

Although not given much attention, observation (b) is evident in the work of many authors (Hayes et al., 1991; Zhang et al., 1995; Sprycha, 1989a, 1989b). This apparently does not arise from the selection of ΔpK_a value, because, Hayes et al. (1991) who investigated three oxides including alumina at different values of ΔpK_a, still observed the same behaviour. It therefore appears that, it is difficult to model both the positively and negatively charged surface of an oxide using the same values of adjustable parameters. The underlying problem for this observation may be due to the assumption that C_1 is constant through out the pH range. Since values of σ_0 are normally

very sensitive to C_1, its slight variation may result in a significant effect on the predicted values of σ_0. Hence if C_1 is expressed as a function of pH, then different values of C_1 may be used for the positively and negatively charged surface. If this modification were to be incorporated in the model, it would certainly be possible to model the two surfaces with the varying values of C_1. The problem, however, is how to obtain the $C_1 = f(pH)$ relationship. The physical approach towards elucidating this relationship would to be to model values of σ_0 above PZC separately to those below PZC. This would provide two values of C_1 that adequately fit the data at the extremes of their respective ranges. These values would represent limits useful in the elucidation of the $C_1 = f(pH)$ relationship.

Variation of C_1 With Type of Electrolyte

The optimal values of C_1 at various c_0 (Table 3) are plotted as a function of $-\log c_0$ in Figure 13 for all electrolytes studied. From this it can be seen that:

a) For all chlorides and nitrates studied, C_1 generally decreases with decrease in c_0.

b) At high c_0 ($c_0 \geq 10^{-1}$ M), C_1 decreases according to the following order of cations Na$^+$
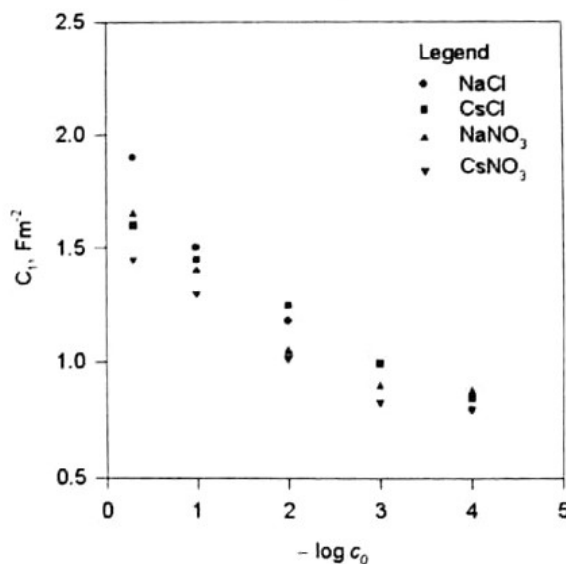

Figure 13: C_1 as a function of $-\log c_0$ for various electrolytes studied

78

Uhandisi Journal Vol. 26, No. 2, December 2003

> Cs$^+$.

c) At extreme low c_0 ($c_0 \approx 10^{-4}$ M), the values of C_1 for all electrolytes appear to converge at the same value (0.85 ± 0.02 Fm^{-2}).

Observation (a) indicates that at high c_0 the concentration of ions in the suspension is relatively high compared to that at low c_0 and consequently more ions are attracted to the surface of the particle resulting to the high values of C_1 than that at low c_0. Assuming that the effect of screening the charge with a chloride ion is the same in NaCl and CsCl, then the variations of C_1 at constant c_0 are essentially due to the effect of cations. The observed decreasing trend of C_1 (observation (b)) suggests that cations with large ionic size are less attracted to the surface compared to those with small ionic size. This observation may be described in terms of the hydrated ionic radii of cations and their tendency to loose their water of hydration as they approach the surface.

Observation (c) suggests that at low c_0 ($c_0 \approx 10^{-4}$

M), the variations in C_1 are not so pronounced. The limiting value of C_1 (0.85 Fm^{-2}) has uncertainty of 2%, indicating that the values are adequately close. It is therefore apparent that at extreme low values of c_0 the amount of ions attracted to the particle surface is independent of the type and the hydrated ionic size of cations.

Effect of Variation of Adjustable Parameters on Goodness of Fit

The results of variation of C_1 and $p\phi$ on the goodness of fit parameter (V_Y) for NaCl are presented in Table 4. Similar results were obtained for other electrolytes studied. From Table 4 it can be seen that

values of V_Y are generally very sensitive to change in C_1 rather than to change in $p\phi$. The predicted values of σ_0 are consequently more sensitive to variation in C_1 than in $p\phi$. It is evident that at a given c_0 and constant value of $p\phi$ variation of C_1 results in V_Y passing through a minimum value, where the fit of the model is best. Away from this value, V_Y continues to rise indicating that the fit is

Table 4 Effect of variation of C_1 and $p\phi$ on V_Y at various concentrations of NaCl.

c_0 (mol/l)	C_1 (Fm^{-2})	$p\phi$	V_Y
10^{-1}	1.6	0	15.66
	1.5	0	0.50
	1.45	0	11.93
	1.5	-0.1	28.42
	1.5	0.1	15.36
10^{-2}	1.2	0.3	5.92
	1.18	0.3	0.29
	1.15	0.3	5.37
	1.18	0.1	82.24
	1.18	0.2	23.04
10^{-3}	1.05	0.3	22.01
	1.0	0.3	1.11
	0.95	0.3	47.59
	1.0	0.1	51.87
	1.0	0.2	9.41
10^{-4}	0.85	0.3	8.32
	0.80	0.3	0.24
	0.75	0.3	9.91
	0.80	0.1	52.35
	0.80	0.4	8.25

poor. Variation of $p\phi$ at constant C_1 and c_0 results in a similar effect, but less pronounced. The best fits of experimental data were therefore obtained when the V_Y value fell within the range $0.1 \leq V_Y \leq 10$.

CONCLUSIONS

In this study, experimental values of σ_0 as a function of pH have been processed using a TLM. Model parameters were obtained using procedures described herein. The inner layer capacitance (C_1) and a negative logarithmic parameter ($p\phi$) were given prescribed (adjustable) values. The overall variance (V_Y) suggested by Dzombak and Morel (1990); Hayes et al. (1991); Katz and Hayes (1995) was used to indicate the good fit between experimental and predicted values of σ_0. It was observed that, for the pH range of $3.5 \leq pH \leq 11.0$ and $10^{-4} \leq c_0 \leq 0.1$ M, best fits (within $\pm 10\%$) were obtained using C_1 in the range of $0.8 \leq C_1 \leq 2.0$ Fm^{-2} and $p\phi$ in the range of $-0.5 \leq p\phi \leq 0.3$ for all electrolytes investigated. This range of C_1 is within the optimal range of this parameter (0.1-2.0 Fm^{-2}) suggested by Hayes et al. (1991).

It was also observed that, for all electrolytes studied optimal values of C_1 decreased with decrease in c_0. At $c_0 \geq 10^{-1}$ M, values of C_1 decrease according to the following order of cations Na$^+$ > Cs$^+$ whereas at $c_0 \approx 10^{-4}$ M, values of C_1 converged to a value of 0.85 Fm^{-2}. At low c_0, the amount of ions attracted to the particle surface appears to be independent of the type of electrolyte and the hydrated size of cations.

A sensitivity analysis carried out on all electrolytes studied indicates that the predicted values of σ_0 are much more sensitive to variation of C_1 rather than $p\phi$.

The TLM suggested herein can adequately predict σ_0 within $\pm 10\%$ accuracy for a wide range of c_0.

From this work following conclusions can be drawn:

a) The data presented herein augment the available data of α-alumina and provide a resource for surface modeling.

b) The absolute values of σ_0 increases with increase of c_0 and it decreases with decrease in c_0.

c) The TLM adequately predicts σ_0 over the range $3 \leq pH \leq 11$, $10^{-4} \leq c_0 \leq 0.1$ M to usually better than $\pm 10\%$.

d) Values of C_1 decrease with decrease in c_0. At constant c_0, they vary with the type of electrolyte.

e) The polarity of the values of σ_0 can be varied through zero by varying pH of the suspension.

NOMECLATURE

A_{sp}	Specific surface area m^2/g
c_0	Electrolyte concentration mol/l
c_s	Oxide concentration g/l
C_1	Capacitance of the Inner layer Fm^{-2}
C_2	Capacitance of the Outer layer Fm^{-2}
e	Electronic charge C
k	Boltzmann constant JK^{-1}
K_{a1}	Acid Intrinsic dissociation constant -
K_{a2}	Base Intrinsic dissociation constant -
K_{An}	Anion intrinsic dissociation constant -
K_{Cat}	Cation intrinsic dissociation constant -
M	Element of the mineral oxide e.g. Al, Fe, etc.-
m_p	Mass of the particle g
N_{AL}	Moles of reagent consumed by sample (alumina) titration μmol
N_{BL}	Moles of reagent consumed by blank titration μmol
N_p	Number of data points-
N_R	Number of components for which the total and free concentrations are known -

N_s — Surface density of adsorption sites sites/nm^2

N_u — Number of adjustable parameters-

R — Gas constant JK^{-1}mol^{-1}

S_i — Estimated error for i^{th} titration data point -

T — Absolute temperature K

V_Y — Overall variance -

Y_i — Residuals for i^{th} data point -

σ'' — Analytical (titratable) surface charge μCcm^{-2}

σ_0 — Absolute surface charge density μCcm^{-2}

σ_s — Initial surface charge μCcm^{-2}

ψ_0 — Surface potential mV

Subscripts β and d, refer to the distances from the particle surface. *Cat* and *An* represent Cation and Anion, respectively.

ABBREVIATIONS

BET — Brunauer, Emmett and Teller

CIP — Common Intersection Point

DF — Degree of Freedom

PSD2 — Precision Syringe Drive (2 modules)

PZC — Point of Zero Charge

SOS — Sum of Squares

TLM — Triple Layer Model

REFERENCES

1. Cesarano, J., Aksay, I.A. and Bleier, A., *Stability of Aqueous α-Al₂O₃ Suspensions with Poly (methacrylic acid) Polyelectrolyte*, J. Amer. Ceram. Soc., Vol. 71 No. 4, pp. 250-255, 1988.

2. Davis, J. A. and Leckie, J. A., *Surface Ionisation and Complexation at the Oxide/Water Interface*, J. Colloid and Interface Sci., Vol. 74 No. 1, pp. 32-43, 1980.

3. Davis, J. A. and Leckie, J. O., *Surface Ionisation and Complexation at the Oxide/Water Interface, II. Surface Properties of Amorphous Iron Oxyhydroxide and Adsorption of Metal Ions*, J. Colloid and Interface Sci., Vol. 67 No. 1, pp. 90-107, 1978.

4. Davis, J.A., James, R.O. and Leckie, J.O., *Surface Ionisation and Complexation at the Oxide/Water Interface, I. Computation of Electric Double Layer Properties in Simple Electrolytes*, J. Colloid and Interface Sci., Vol. 63, No. 3, pp. 480-499, 1978.

5. Dzombak, D. A. and Morel, F. M. M., *Surface Complexation Modeling: Hydrous Ferric Oxide*, pp. 120-140, Wiley-Interscience Publishers, New York, 1990.

6. Hayes, K. F., Redden, G., Ela, W. and Leckie, J. O., *Surface Complexation Models: An Evaluation of model Parameter Estimation Using FITEQL and Oxide Mineral Data*, J. Colloid and Interface Sci., Vol. 142 No.2, pp. 448-469, 1991.

7. Huang, C.P. and Stumm, W., *Specific Adsorption of Cations on Hydrous γ-Al₂O₃*, J. Colloid and Interface Sci., Vol. 43 No. 2, pp. 409-420, 1973.

8. Huang, C.P., *The Surface Acidity of Hydrous Solids*, In *Adsorption of Inorganics at Solid-Liquid Interfaces*, pp.183-217, (Eds. Anderson, M. A. and Rubin, J. A.), Ann Arbor Science, Ann Arbor, Michigan, 1981.

9. Hunter, R. J., *Foundations of Colloid Science*, Vol. 1, pp. 245-260, Oxford University Press, New York, 1993.

10. Hunter, R. J., *Introduction to Modern Colloid Science*, pp. 230-254, Oxford University Press, New York, 1996.

11. James, R. O. and Parks, G. A., *Characterisation of Aqueous Colloids by Their Electric Double Layer and Intrinsic Surface Chemical Properties*, In *Surface and Colloid Science*, Vol. 12, pp. 119-217 (Ed. Matejevic, E.), Plenum, New York, 1982.

12. Katz, L. E. and Hayes, K. F., *Strategy for Modeling Monomer Complex Formation at Moderate Surface Coverage*, J. Colloid and Interface Sci., Vol. 170 No. 4, pp. 477-490, 1995.

13. Koopal, L. K., van Riemsdijk, W. H. and Roffey, M. G., *Surface Ionisation and Complexation Models: A Comparison of Methods for Determining Model Parameters*, J. Colloid and Interface Sci., Vol. 118 No. 1, pp.117-136, 1987.

14. Lutzenkirchen, J. Magnico, P. and Behra, P., *Constraints upon Electrolyte Binding Constants in Triple Layer Calculations and Consequences of the Choice of the Thermodynamic Framework*, J. Colloid and Interface Sci., Vol. 170 No. 2, pp.326-334, 1995.

15. Lutzenkirchen, J., *Parameter Estimation for Constant Capacitance Complexation Model: Analysis of Parameter Interdependences*, J. Colloid and Interface Sci., Vol. 210 No. 3, pp.384-390, 1999.

16. Lutzenkirchen, J., *Parameter Estimation for the Triple Layer Model: Analysis of Conventional Methods and suggestion of alternative possibilities*, J. Colloid and Interface Sci., Vol. 204 No. 1, pp.119-127, 1998.

17. Lyklema, J., *Fundamentals of Interface and Colloid Science*, Vol. II, pp. 280-302, Academic Press, London, 1995.

18. Mustafa, S., Dilara, B., Neelofer, Z., Naeem, A. and Tasleem, S., *Temperature Effect on the Surface Charge Properties of γ-Al_2O_3*, J. Colloid and Interface Sci., Vol. 204 No. 2, pp. 284-293, 1998.

19. Ntalikwa, J.W., Bryant, R. and Zunzu J.S.M., *Electrophoresis of Colloidal α-alumina*, J. Colloid and Polymer Sci., Vol. 279 No. 4, pp 843-849, 2001.

20. Pivovarov, S., *Surface Structure and Site Density of the Oxide-Solution Interface*, J. Colloid and Interface Sci., Vol. 196 No. 3, pp. 321-323, 1997.

21. Schindler, P. W., *Surface Complexes at Oxide-Water Interfaces*, In *Adsorption of Inorganic at Solid-Liquid Interfaces*, pp.1- 49, (Eds. Anderson, M. A. and Rubin, J. A.), Ann Arbor Science, Ann Arbor, Michigan, 1981.

22. Smit, W. and Holten, C. L., *Zeta Potential and Radio Tracer Adsorption Measurements on EFG α-Al_2O_3 Single crystals in NaBr Solutions*, J. Colloid and Interface Sci., Vol. 78 No.1, pp. 1-14, 1980.

23. Sprycha, R., *Electric Double Layer at Alumina/Electrolyte Interface, I. Surface Charge and Zeta Potential*, J. Colloid and Interface Sci., Vol. 127 No. 1, pp. 1-11, 1989a.

24. Sprycha, R., *Electric Double Layer at Alumina/Electrolyte Interface, II. Adsorption of Supporting Electrolyte Ions*, J. Colloid and Interface Sci., Vol. 127 No. 1, pp. 12-24, 1989b.

25. Stumm, W. and Morgan, J. J., *Aquatic Chemistry: An Introduction Emphasizing Chemical Equilibria in Natural Waters*, pp. 345-365, Wiley-Interscince Publishers, New York, 1981.

26. Wiese, G. R. and Healy, T. W., *Coagulation and Electrokinetic Behaviour of TiO_2 and Al_2O_3 Colloidal Suspensions*, J. Colloid and Interface Sci., Vol. 51 No. 3, pp. 427-433, 1975.

27. Yates, D. E, Levine S., and Healy, T. W., *Site-Binding Model of the Electric Double Layer at the Oxide/ Water Interface*, J. Chem. Soc. Faraday Trans., Vol. 70, No. 4, pp. 1807-1822, 1974.

28. Zhang, Q., Xu, Z., and Finch, J. A., *Surface Ionisation and Complexation at the Sphalerite/Water interface, I. Computation of Electric Double Layer Properties of Sphalerite in a Simple Electrolyte*, J. Colloid and Interface Sci., Vol. 169 No. 3, pp. 414-421, 1995.

29. Zhang, Z. Z., Sparks, D. L. and Scrivner, N. C., *Characterisation and Modeling of Al-Oxide/Aqueous solution Interface, I. Measurement of Electrostatic Potential at the Origin of the Diffuse Layer Using Negative Adsorption of Na^+ Ions*, J. Colloid and Interface Sci., Vol. 162 No. 2, pp. 244-251, 1994.